Rare Metal Materials and Engineering
Volume 54, Issue 11, November 2025
Available online at www.rmme.ac.cn

Science Press

Cite this article as: Hao Qingrui, Li Yongquan, Li Ning, et al. Microstructure and High-Temperature Oxidation Resistance of Cr-Al-Y Co-deposition Coating on TiAlNb9 Alloy Surface[J]. Rare Metal Materials and Engineering, 2025, 54(11): 2739-2748. DOI: https://doi.org/10.12442/j.issn.1002-185X.E20240572.

ARTICLE

Microstructure and High-Temperature Oxidation Resistance of Cr-Al-Y Co-deposition Coating on TiAlNb9 Alloy Surface

Hao Qingrui[1], Li Yongquan[2,3], Li Ning[1], Gao Yang[2]

[1] School of Materials Science and Engineering, North Minzu University, Yinchuan 750021, China; [2] College of Mechatronic Engineering, North Minzu University, Yinchuan 750021, China; [3] Ningxia Engineering Research Center for Hybrid Manufacturing System, Yinchuan 750021, China

Abstract: To improve the high-temperature oxidation resistance of TiAlNb9 alloy, a Cr-Al-Y co-deposition coating was prepared on the alloy surface by the pack cementation method. The microstructure of the coating was analyzed by scanning electron microscope, energy dispersive spectrometer, and X-ray diffractometer, and the high-temperature oxidation properties of the substrate and coating at 1273 K were compared and studied. The results show that the Cr-Al-Y coating is about 30 μm in thickness, and it has a dense structure and good film-substrate bonding. The coating includes an outer layer composed of $TiCr_2$, TiCr, Ti_4Cr, and $(Ti,Nb)Cr_4$ phases as well as an inner layer composed of Ti_2Al, and Nb-rich γ-TiAl interdiffusion zone. The TiAlNb9 substrate forms an oxide layer composed of TiO_2 and Al_2O_3 at 1273 K. Due to its loose and porous structure, TiO_2 oxide film cannot effectively isolate the internal diffusion of element O, resulting in continuous oxidation damage to the substrate. The Cr-Al-Y co-deposition coating forms a dense Cr_2O_3 and Al_2O_3 oxide layer during oxidation, effectively preventing the internal diffusion of element O and significantly improving the high-temperature oxidation resistance of the substrate alloy.

Key words: pack cementation; TiAlNb9 alloy; Cr-Al-Y co-deposition coating; high-temperature oxidation resistance

1 Introduction

TiAl-based alloys not only have the advantages of low density and high specific strength of ordinary TiAl alloys, but also have better high-temperature properties such as oxidation and creep resistance. They are widely used in high temperature components such as engine compressors and turbine blades in the aerospace field[1–2]. At high temperature above 1073 K, the oxide layer formed on the surface of TiAl alloy cannot effectively prevent the continuous erosion of element O on the alloy, which seriously affects its service temperature and service life[3]. Anti-oxidation coating[4–5] is prepared on the surface of the alloy by surface modification technique, which can form a dense oxide film during oxidation and effectively hinder the erosion of element O. At the same time, the cost is relatively low, the process flow is relatively simple, and the performance of the original alloy can be retained to the maximum extent, so it is widely used.

In recent years, many researchers have done a lot of research on anti-oxidation coatings. Rojas et al[6] deposited Cr-Al-N coatings on M2 steel, which show excellent oxidation resistance at 1273 K. Richter et al[7] prepared Al-Si composite coating on binary transition metal (diboride) by reactive arc evaporation technique, and results showed that the coating has excellent oxidation resistance at 1473 K. Wu et al[8] deposited a diffusion aluminum coating on the surface of TiAl alloy by electron beam physical vapor deposition technique and formed a dense Al_2O_3 oxide film on the surface of substrate at high temperatures, which greatly improved the oxidation resistance of the alloy. Zhang et al[9] prepared an aluminized modified coating on γ-TiAl alloy by pack cementation. The thickness of the coating is up to 70 μm, and the coating is closely combined with the substrate, significantly improving the oxidation resistance in a high-temperature environment.

The above research shows that the aluminide coating can

Received date: November 01, 2024
Foundation item: National Natural Science Foundation of China (52161009); Innovation Project of Postgraduate Students in North Minzu University (YCX24104)
Corresponding author: Li Yongquan, Ph. D., Associate Professor, College of Mechatronic Engineering, North Minzu University, Yinchuan 750021, P. R. China, E-mail: 2014141@nmu.edu.cn

form an effective protective coating on the surface of TiAl-based alloy, thereby improving the high-temperature performance of the alloy. However, the $TiAl_3$ phase formed on the pure aluminized coating is more brittle[10], and it is easy to produce penetrating cracks under high-temperature conditions, resulting in the spalling of aluminized coating and accelerating the failure of protective coating. Ref. [11 – 12] showed that adding element Cr to the Al coating not only improves the bonding force between coating and substrate as well as the strength of coating, but also plays a role in improving the compactness of the oxide layer during oxidation, thereby more effectively preventing the internal diffusion of element O. In addition, rare earth element Y with the 4f orbit has a strong adsorption effect on active atoms, which can effectively promote the diffusion of active atoms such as Cr and Al, refine the grains, and enhance the anti-stripping ability of the coating[13–15]. In this study, the Cr-Al-Y co-deposition coating was prepared on the surface of TiAlNb9 alloy by pack cementation. The microstructure of the Cr-Al-Y coating was analyzed, and the oxidation behavior and oxidation mechanism of TiAlNb9 alloy and Cr-Al-Y coating at 1273 K were investigated.

2 Experiment

Fig. 1 shows the process flow diagram of pack cementation and the schematic diagram of the device for preparing the Cr-Al-Y coating. The experimental sample was TiAlNb9 alloy with the dimension of 7 mm×7 mm×2 mm, and the main chemical composition was Ti-35Al-9Nb (at%). The samples were first polished with different specifications of SiC sandpaper (400# – 3000#), then washed, and dried. The composition of the infiltration agent was optimized to be 4Al-10Cr-2Y_2O_3-6NH_4Cl-78Al_2O_3 (wt%), in which Al and Cr are powder with a purity of 99.9wt%, Y_2O_3 provides rare earth elements, NH_4Cl is a catalyst, and Al_2O_3 is an inert filler. The pretreated sample was placed in a corundum crucible with a penetrating agent, and the crucible was sealed with a solid binder. After standing for 12 h, it was placed in a vacuum furnace and heated to 1323 K with the furnace. After holding for 2 h, the crucible was taken out and air-cooled to room temperature. Scanning electron microscope (SEM, German Zeiss SIGMA 500) and energy dispersive spectrometer (EDS) were used to observe and analyze the surface and cross-section morphologies and element distribution of the co-deposition coating. X-ray diffractometer (XRD, XRD-6000, 3KW) was used to analyze the phase composition of the coating.

The SX2-5-12A box-type resistance furnace was heated to 1273 K, and the TiAlNb9 alloy and the Cr-Al-Y coating sample were placed in the resistance furnace. The sample was taken out and air-cooled to room temperature every certain time (4 h). The FA1004 electronic analytical balance (0.1 mg) was used to weigh the sample with a crucible. The oxide film would peel off, so the crucible was weighed, and was calcined before the experiment. The mass change data of sample were recorded. This step was repeated until the end of the experiment. To reduce the experimental error, five groups of parallel experiments were conducted, and the average value was obtained. The microstructure and composition of the substrate and the coating after oxidation were characterized by XRD, SEM, and EDS, and the oxidation mechanism was analyzed.

3 Results and Discussion

3.1 Microstructure of Cr-Al-Y co-deposition coating

Fig. 2a shows the surface morphology of the Cr-Al-Y co-deposition coating. It can be seen that the surface of the coating prepared at 1323 K for 2 h is dense and smooth, and there are fine black $TiCr_2$ particles in localized areas. The cross-section morphology in Fig. 2c shows that the thickness of the coating is about 30 μm, the structure is uniform and dense. There is obvious stratification, and the layers are tightly bonded. The thickness of the outer layer (number 1) is about 17 μm, and it is light gray. EDS element distribution mapping in Fig.2e shows that the element Cr in the outer layer is rich. Combined with the analysis of XRD patterns, the outer layer is mainly composed of $TiCr_2$, TiCr, (Ti, Nb)Cr_4, and Ti_4Cr phases. The thickness of inner layer (number 2) is about 6 μm, and it is dark gray. The inner layer is rich in element Al. The elemental concentration distribution curves in Fig. 2d shows that the Ti: Al ratio is about 2: 1. Combined with the XRD pattern analysis in Fig.2b, it could be seen that the inner layer is Ti_2Al phase. The thickness of the interdiffusion zone (number 3) is about 7 μm, which is composed of striped bright

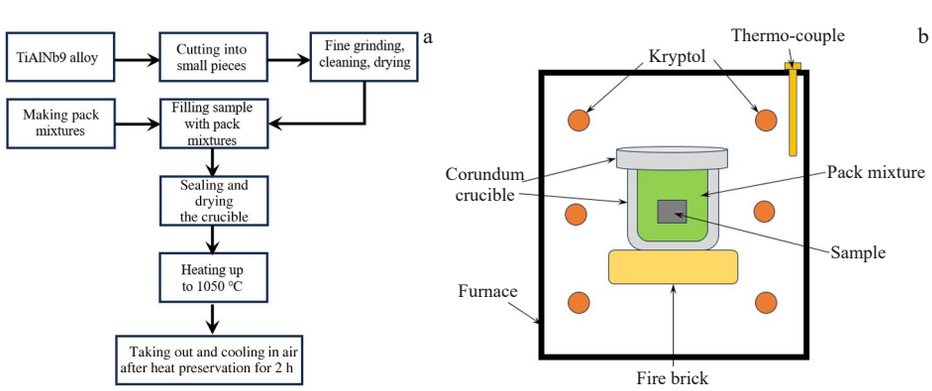

Fig.1 Process flow diagram of pack cementation (a) and schematic diagram of device for preparing Cr-Al-Y coating (b)

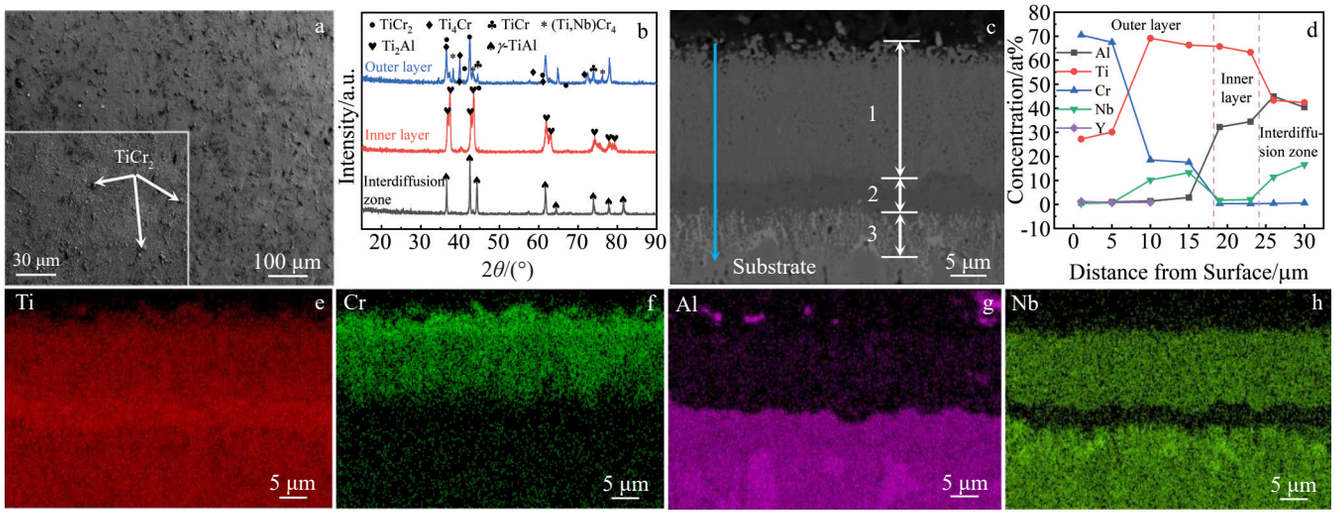

Fig. 2 Surface morphology (a), XRD patterns from outer layer to interdiffusion zone (b), cross-section morphology (c), and elemental concentration distribution curves (d) of Cr-Al-Y co-deposition coating; EDS element mappings corresponding to Fig.2c (e–h)

white structure and dotted dark gray structure. The content of element Nb in interdiffusion zone is significantly higher than that in other layers. Combined with the Ti-Al binary phase diagram[16], it could be seen that the dotted dark gray structure in the interdiffusion zone is γ-TiAl phase, and the striped bright white structure is Nb-rich γ-TiAl phase. It is worth noting that the element Y only exists in the outer layer, and its content is very small. Except for the outer layer, the element Y is not detected in other layers, and there is no diffraction peak of the related compound phase of Y in XRD pattern. This might be because Y is dissolved in Ti-Cr or Ti-Al compounds, or the compound content of Y is very small.

3.2 High-temperature oxidation property

3.2.1 Oxidation kinetics of TiAlNb9 alloy and Cr-Al-Y coating at 1273 K

Fig. 3 shows the oxidation kinetics curves of TiAlNb9 alloy and Cr-Al-Y coating at 1273 K and the statistical diagram of oxide layer thickness at different oxidation times. Fig. 3a shows that the mass gain of the substrate is relatively slow at the initial stage of oxidation, and it rises sharply after 20 h, reaching 9.23 mg/cm^2 at 52 h. The mass gain rate of the Cr-Al-Y coating is relatively high at the initial stage of oxidation and also changes around 20 h. After that, the mass gain tends to be gentle, which is only 2.49 mg/cm^2 at 52 h. It could be seen from Fig. 3b that under the same oxidation time, the oxide layer thickness of the substrate is much larger than that of the coating. And the oxide layer thickness of the substrate reaches about 60 μm after oxidiation for 10 h, while the thickness of the coating is about 20 μm. The above phenomena indicate that the Cr-Al-Y coating has a significant protective effect on the TiAlNb9 alloy under high-temperature conditions.

3.2.2 High-temperature oxidation of TiAlNb9 alloy at 1273 K

Fig. 4 shows the surface morphologies and XRD patterns of TiAlNb9 alloy after oxidation at 1273 K for 0.5, 5, and 10 h. Fig. 4a shows that the substrate surface after high-temperature oxidation for 0.5 h is dark gray on the whole with some light gray areas, and the dark gray area is relatively flat. EDS analysis combined with XRD patterns in Fig. 4d shows that the main components in this area are TiO_2 and a small amount of TiO. The enlarged image of the light gray area shows that there are obvious bulges and spalling, the surface particles are strong, and the density is poor. The EDS result of Area 2 shows that the main components include Al_2O_3 and TiO_2. Compared with the unpeeled zone (Areas 1 and 2), the content

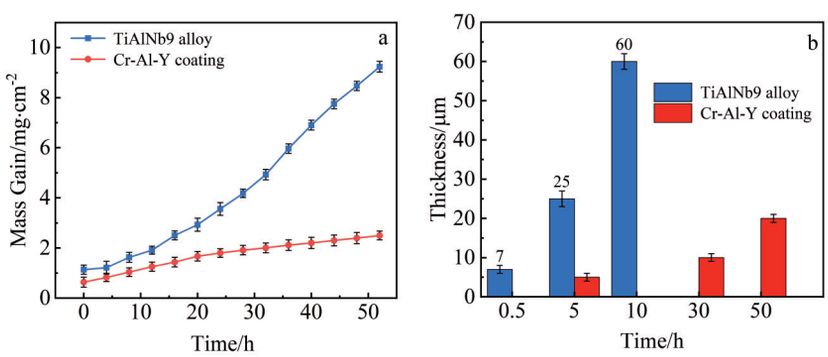

Fig. 3 Oxidation kinetics curves (a) and oxide layer thickness (b) of TiAlNb9 alloy and Cr-Al-Y co-deposition coating at 1273 K

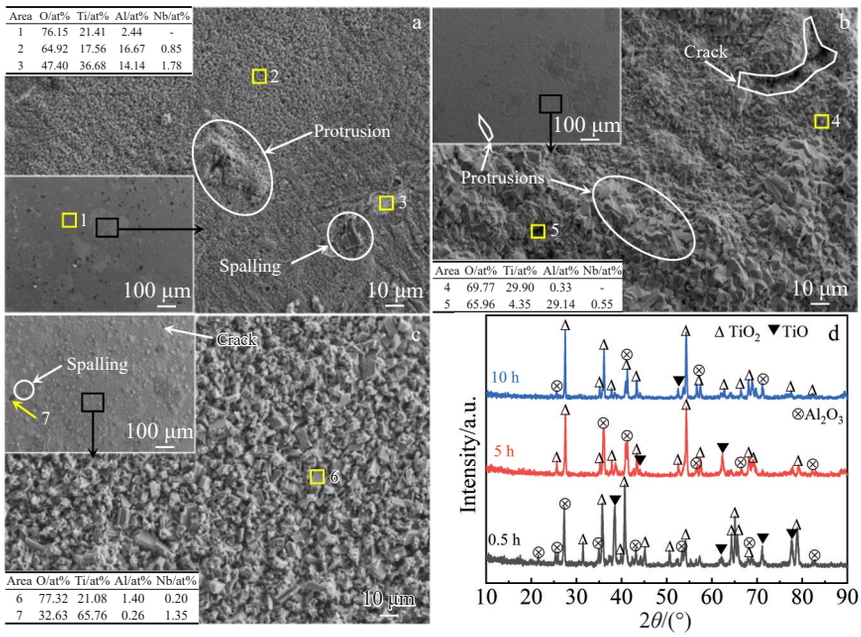

Fig.4 Surface morphologies with corresponding EDS results (a–c) and XRD patterns (d) of TiAlNb9 alloy after oxidation at 1273 K for different time: (a) 0.5 h, (b) 5 h, and (c) 10 h

of element Ti increases by about 71% and the content of element Nb increases significantly after the peeling of the light gray structure (Area 3), indicating that the TiAlNb9 alloy is not completely oxidized below the peeling zone.

Fig.4b shows that after high-temperature oxidation for 5 h, a large number of worm-like bulges are formed on the substrate surface in the upper left corner. The enlarged image shows that the substrate surface is stacked by gray cubic particles with different sizes, and there are obvious internal propagation cracks, while the accumulation of large particles forms a worm-like bulge on the surface of substrate. EDS result of Area 4 and XRD analysis show that the cubic particle structure is TiO_2, the content of element Al at the crack (Area 5) is 29.14at%, and the main components are Al_2O_3 and TiO_2.

In Fig.4c, the substrate surface after high-temperature oxidation for 10 h has obviously changed compared with that before oxidation. It could be seen from the low-magnification morphology in the upper left corner that there is a clearly visible granular structure with cracks and flaking, and the density is poor. The massive particle structure in the enlarged image is composed of TiO_2 and a small amount of Al_2O_3. The composition of the spalling zone shown in Area 7 is mainly TiO_2.

Fig. 5 shows the cross-sectional morphologies of TiAlNb9 alloy after oxidation at 1273 K for 0.5, 5, and 10 h and EDS element mappings corresponding to Fig. 5c. Table 1 shows EDS results of typical phases marked in Fig. 5. Fig. 5a shows that after high-temperature oxidation for 0.5 h, an oxide layer with a thickness of about 7 μm is formed on the substrate surface. The structure of the oxide layer is loose, some areas are peeled off, and obvious cracks appear at the junction with the substrate. The EDS result shows that the oxide layer is a mixed phase of TiO_2 and Al_2O_3. The content of element Ti in the upper part of the oxide layer (Area 8) is higher than that of element Al, and the opposing situation occurs in the region near the substrate (Area 9).

Fig. 5b shows that the thickness of the oxide layer on the substrate surface increases to 25 μm after high-temperature oxidation for 5 h, and obvious stratification occurs. The outer layer is light gray, and the inner layer is dark gray. There are transverse holes at the interface between the outer layer and the inner layer. The cubic granular structure can be seen on the upper part, which is consistent with the worm-like bulge structure in Fig. 4b. The outer layer (Area 10) is mainly composed of TiO_2, and the inner layer (Area 11) is mainly composed of Al_2O_3. EDS result of Area 12 shows that the content of element Ti in the embedded structure is significantly higher than that in the inner layer. According to analysis, the structure is a mixed phase of Al_2O_3 and TiO_2, and the content of TiO_2 is relatively high. Therefore, the color is different from the dark gray color of the inner layer, but presents a light gray close to the outer layer.

In Fig. 5c, the thickness of oxidation layer after 10 h of high-temperature oxidation increases to about 60 μm, and the stratification is similar to that after 5 h. The obvious difference is that the proportion of the inner layer increases significantly and that of the middle layer decreases. The outer layer shows irregular particle stacking, which is consistent with the obvious increase in pores and cracks in Fig.4c. There are many holes and cracks in the middle layer connecting the outer layer, and the binding force is poor. The inner layer is filled with small holes, and a large number of holes near the substrate side expand into transverse cracks.

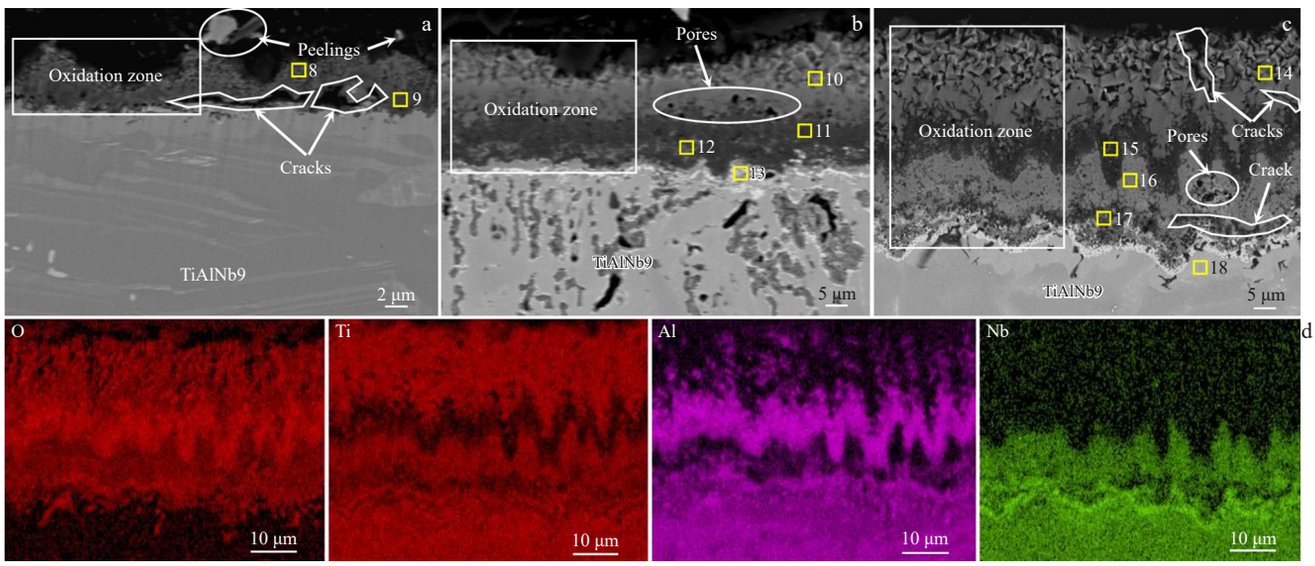

Fig.5 Cross-sectional SEM images of TiAlNb9 alloy after oxidation at 1273 K for 0.5 h (a), 5 h (b), and 10 h (c); EDS element mappings corresponding to Fig.5c (d)

Combined with Table 1 and Fig.5d, the outer layer (Area 14) mainly contains elements O and Ti, indicating the TiO_2 phase. The middle layer (Area 15) is rich in element Al, and the content of Ti is rare. The composition is mainly Al_2O_3 phase. The inner layer (Area 16) is a mixed phase of TiO_2 and Al_2O_3. The content of element Nb increases obviously. A large amount of element Al is enriched at the crack (Area 17), and the content of element Nb in Area 18 reaches 19.48at%, indicating that the element Nb inside the substrate diffuses outward.

In Fig. 5b, the content of element O at the junction of the substrate and the oxidation layer (Area 13) reaches 41.15at%, and element O is also detected in Area 18 (Fig.5c). And it can be seen from Fig. 5d that element O has diffused to the substrate after oxidation for 10 h, indicating that the surface oxidation layer produced by oxidation of TiAlNb9 alloy cannot prevent the internal diffusion of element O.

Table 1 Chemical composition of areas marked in Fig.5

Area	Element/at%			
	O	Ti	Al	Nb
8	67.79	20.42	11.15	0.64
9	61.90	10.55	24.91	2.64
10	63.13	34.68	1.76	0.43
11	58.15	0.47	39.81	1.57
12	39.75	28.53	17.60	14.12
13	41.15	19.73	24.85	14.27
14	70.55	28.80	0.65	-
15	61.24	3.84	34.76	0.16
16	66.39	27.14	3.03	3.44
17	61.84	4.92	31.17	2.07
18	21.10	31.52	27.90	19.48

3.2.3 High-temperature oxidation mechanism of TiAlNb9 alloy at 1273 K

At the initial oxidation stage of TiAlNb9 alloy, TiO_2 and Al_2O_3 nucleate at the same time, because the thermodynamic stabilities of TiO_2 and Al_2O_3 are similar. However, the lattice structure of TiO_2 has strong disorder, resulting in its growth rate being much larger than that of Al_2O_3. Therefore, the early oxidation layer is mainly composed of TiO_2, and the diffused element Al is enriched below the oxidation layer, which promotes the formation of subsequent Al_2O_3[17–19]. At the same time, Al has a certain solubility in TiO_2[20]. The element Al enriched below the oxidation layer will gradually diffuse to the TiO_2 layer and combine with O to form Al_2O_3, which is dark gray within the oxidation layer shown in Fig. 5b. In the subsequent oxidation process, the TiO_2-dominated and Al_2O_3-dominated oxidation layers are alternately generated and stacked to form an oxide product layer with a composite structure. As shown in Fig.5c, after 10 h of oxidation, a TiO_2 oxidation layer is formed under the Al_2O_3 oxidation layer, and a large amount of element Al is enriched at the transverse cracks inside the newly formed TiO_2 oxidation layer. According to the growth process of the oxidation layer, it can be inferred that this area is a new Al_2O_3 oxidation layer to be formed.

The application of the alloy under high-temperature conditions depends on the isolation effect of the oxidation products coated on the alloy surface on the element O during the oxidation process. The TiO_2 at high temperature has a rutile structure[21] (tetragonal system, D_4h point group). Under the condition of high oxygen concentration, oxygen vacancy[22] is the main defect. The element O in the air diffuses rapidly to the substrate through the channel formed by the oxygen

vacancy in TiO_2, which provides a necessary condition for the continuous oxidation of elements Al and Ti enriched below the oxidation layer. The single Al_2O_3 oxidation layer has a good density and a positive effect on avoiding alloy oxidation. However, through the analysis of Fig. 5b, it can be seen that the outer layer of the oxidation layer is TiO_2, and the inner layer is composed of TiO_2 and Al_2O_3, which is not a single Al_2O_3 layer and cannot prevent the element O from continuing to diffuse inward. Therefore, TiAlNb9 alloy exposed to high-temperature environment will continue to oxidize and eventually fail. The evolution process of oxidation layer corresponding to different oxidation time of TiAlNb9 alloy is shown in Fig.6.

3.2.4 High-temperature oxidation of Cr-Al-Y coating at 1273 K

Fig.7 shows the surface morphologies and XRD patterns of Cr-Al-Y coating oxidized at 1273 K for 5, 30, and 50 h. The low-magnification morphology in the upper left corner of Fig. 7a shows that the surface of the coating is relatively smooth after 5 h of high-temperature oxidation. There are fine granular and dark gray island structures distributed in the enlarged image. The structure (Area 19) is rich in Al, which is mainly Al_2O_3 phase. The light gray structure (Area 20) contains Cr_2O_3 and TiO_2, and the granular bulge is mainly Cr_2O_3. Some of the bulges are damaged, resulting in punctate spalling. The ratio of Ti to Cr is close to 1:2, and the content of O is 13.83at% in Area 21 after spalling. It might be due to the damage and spalling of the bulge caused by oxidation under the internal stress caused by thermal expansion,

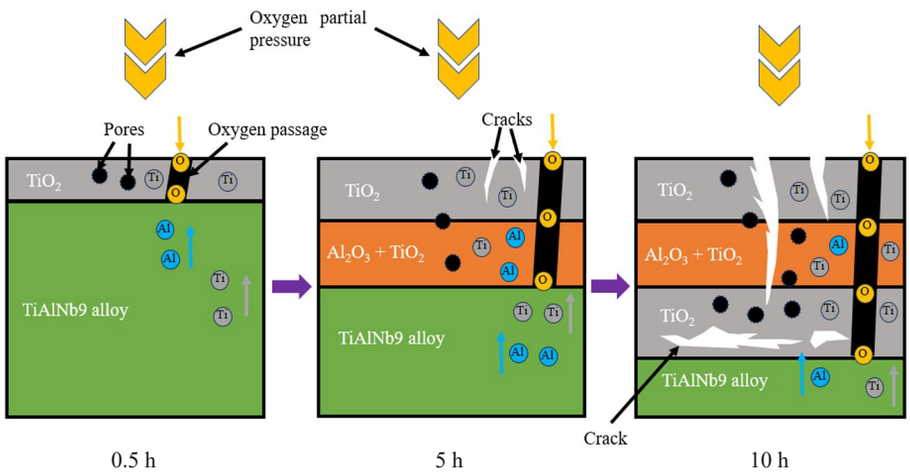

Fig.6 Evolution process of oxidation layer of TiAlNb9 alloy after oxidation at 1273 K for different time

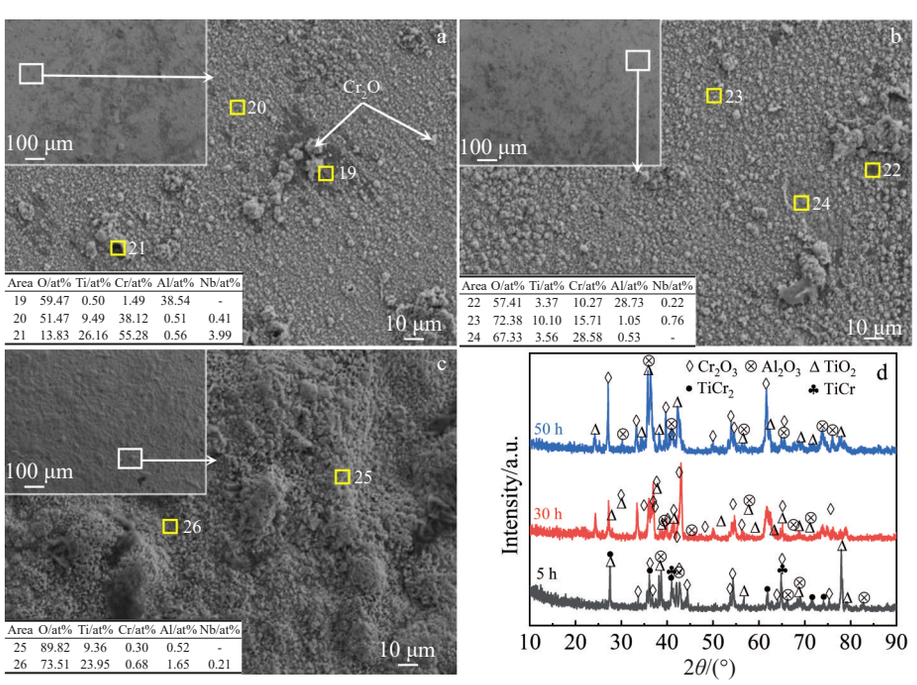

Fig.7 Surface morphologies with corresponding EDS results (a – c) and XRD patterns (d) of Cr-Al-Y coating after oxidation at 1273 K for different time: (a) 5 h, (b) 30 h, and (c) 50 h

exposing the outer layer of the incomplete oxidation layer composed of $TiCr_2$ and TiCr phases.

In Fig.7b, the dark gray structure on the surface of the layer oxidized at high temperatures for 30 h is relatively reduced and more dispersed. EDS analysis of Area 22 shows that the dark gray structure on the surface of the layer oxidized for 30 h is significantly more than that oxidized for 5 h. The content of elements Cr and Ti increases significantly, the content of element Al decreases relatively, and a small amount of element Nb is detected, indicating that the elements in the layer diffused outward with the prolongation of oxidation time. By comparing the enlarged images of Fig. 7a and 7b, it can be seen that the granular protrusions on the surface of the oxidation layer oxidized for 30 h increase significantly, and flake spalling (Area 24) appears. Combined with XRD analysis in Fig.7d, it is found that the main part after spalling is Cr_2O_3, and the Ti content of the oxidation layer is always relatively low, indicating that the oxide product formed on the surface of the oxidation layer is compact, which can effectively prevent the external diffusion of elements inside the oxidation layer.

In Fig. 7c, the surface morphology of the Cr-Al-Y coating after oxidation for 50 h changes significantly compared with that after 30 h, forming the concave and convex morphology. The enlarged image shows that different from the dense surface structure in Fig. 7a – 7b, the surface of coating after 50 h of high-temperature oxidation has net-like structure, which is loose and porous. The O content of the convex part (Area 25) is as high as 89.82at%. The main component is Ti oxide, and the content of elements Al and Cr is very small. The composition of the concave part (Area 26) is the same as that of the convex part. All of them are oxides of Ti, but the content of Al and Cr increases, and element Nb appears, indicating that with the prolongation of oxidation time, the oxidation layer cannot maintain effective density for a long time, resulting in the external diffusion of elements in the layer.

Fig.8 shows the cross-sectional morphologies of the Cr-Al-Y coating after high-temperature oxidation at 1273 K for 5, 30, and 50 h and EDS element mappings corresponding to Fig.8c. The EDS results of the typical phases marked in Fig.8 are shown in Table 2. Fig.8a shows that an oxidation layer of about 5 μm in thickness is formed on the surface of the layer oxidized at high temperature for 5 h. The oxidation layer (Area 27) contains Cr_2O_3, TiO_2, and Al_2O_3, which is consistent with the analysis results in Fig. 7a. Oxygen is not detected below the oxidation layer (Area 28), and the EDS analysis results show that the composition content of this area is similar to that of the outer layer composed of $TiCr_2$ and TiCr phases, indicating that oxygen is blocked in the outer layer of the Cr-Al-Y coating after oxidation for 5 h.

Fig.8b shows that the thickness of the oxidation layer after 30 h of high-temperature oxidation increases to 10 μm, and the upper end of the oxidation layer peels off. The spalling product (Area 29) is analyzed as Cr-rich and Al-rich TiO_2 phases. The product layer with a thickness of about 1 μm at the upper end of the oxidation layer is the same as the spalling product in color and composition. The oxidation product (Area 30) below the spalling layer is mainly Cr_2O_3. No element O is detected in Area 31 below the oxidation layer, indicating that the Cr_2O_3 oxidation layer formed after 30 h of oxidation is dense and uniform, which can effectively prevent the internal diffusion of element O.

In Fig. 8c, the oxidation layer after high-temperature oxidation for 50 h has a great change compared with that before the treatment. Firstly, there is obvious stratification in the structure. The oxidation outer layer is dark gray, and there are obvious holes. The EDS result of Area 32 shows that the dark gray structure is composed of Cr-rich and Al-rich TiO_2 phases, which is consistent with the analysis of oxidation layer surface in Fig. 7c. The oxidation intermediate layer is light gray, and the EDS analysis results of Area 33 show that

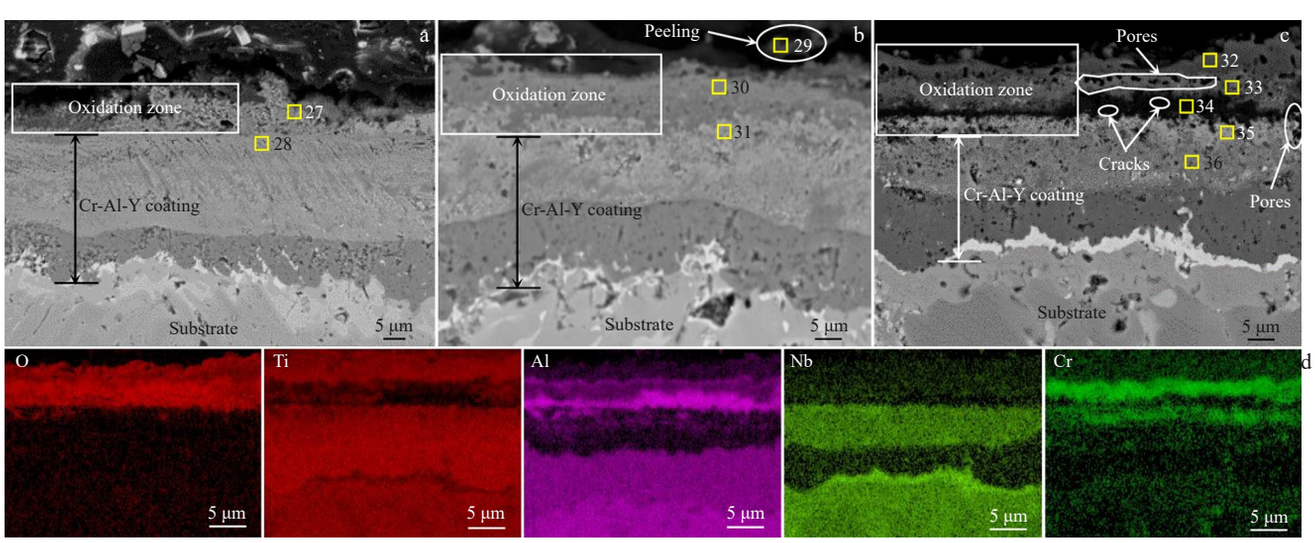

Fig.8 Cross-sectional SEM images of Cr-Al-Y coating after oxidation at 1273 K for 5 h (a), 30 h (b), and 50 h (c); EDS element mappings corresponding to Fig.8c (d)

Table 2 Chemical composition of areas marked in Fig.8

Area	Composition/at%					
	O	Ti	Cr	Al	Nb	Y
27	29.66	9.48	49.62	11.24	-	-
28	-	39.79	51.98	3.25	4.98	-
29	68.96	27.52	2.34	0.97	0.21	-
30	40.42	8.39	46.94	3.42	-	0.83
31	-	72.14	14.88	-	12.98	-
32	74.34	23.65	1.08	0.93	-	-
33	63.85	4.82	21.56	8.94	0.83	-
34	59.59	0.66	1.35	38.40	-	-
35	29.34	27.80	32.21	2.63	8.02	-
36	-	67.37	20.41	0.58	11.64	-

the layer is mainly composed of Cr_2O_3 and Al_2O_3. However, due to long-term oxidation erosion, oxidation intermediate layer (Cr_2O_3 and Al_2O_3) and oxidation outer layer (TiO_2) are combined with a large number of holes, which might subsequently develop into transverse cracks, resulting in the spalling of the oxidation layer. The oxidation inner layer is black-gray, the structure is loose, and a large number of holes are distributed. EDS result of Area 34 shows that there is a large enrichment of element Al. The analysis shows that the black-gray structure is Al_2O_3 phase. Element O is detected below the oxidation layer in Area 35, but it is not detected in Area 36. It shows that the compactness of the surface oxidation layer of the Cr-Al-Y coating after high-temperature oxidation for 50 h is reduced, and the blocking effect on element O is weakened. However, the unoxidized layer can still prevent the internal diffusion of element O, which significantly improves the high-temperature oxidation resistance of TiAlNb9 alloy.

3.2.5 High-temperature oxidation mechanism of Cr-Al-Y coating at 1273 K

In the early stage of oxidation, the element O firstly contacts with the Cr-Al-Y coating, and a large number of Ti and Cr atoms in the outer layer of the coating combine with O to form the corresponding oxides, namely TiO_2 and Cr_2O_3, respectively, which are the main reason for the faster oxidation mass gain rate in the early stage of the coating. Because the free energy of Ti is less than that of Cr, the diffusion rate of Ti atoms is greater than that of Cr atoms[17–18]. Therefore, the content of TiO_2 in the initial oxidation layer is greater than that of Cr_2O_3, while the rutile structure of TiO_2 layer is loose and porous, which cannot effectively prevent the diffusion of element O. With the prolongation of oxidation time, element O diffuses inward through the TiO_2 oxide layer, and a large amount of element Cr diffuses outward in the coating. Under the TiO_2 oxidation layer, element Cr combines with the internally diffused element O to form an oxidation layer dominated by Cr_2O_3 phase. Because element Y enhances the adhesion of the oxide layer under the pinning effect[23], the continuous and dense Cr_2O_3 oxidation layer can effectively hinder the internal diffusion of element O and the external diffusion of element Ti. As shown in the oxidation kinetics curve of coating in Fig.3a, due to the protection of the Cr_2O_3 oxidation layer, the oxidation mass gain rate of the coating tends to be stable in the middle of the test. In addition to the change of the oxidation layer, it can be seen from Fig.8a–8c that the thickness of the inner layer and the interdiffusion zone of the coating increases significantly during the high-temperature oxidation process. This is attributed to the external diffusion of element Al in the substrate at high temperature. This process leads to the formation of Ti_2Al and γ-TiAl phases, which are subsequently deposited into both the inner layer and interdiffusion zone, ultimately resulting in increased thickness.

In the later stage of oxidation, the element Cr continuously diffuses outward to form a Cr_2O_3 oxidation layer, and the remaining vacancies cannot be effectively filled, thus forming an element channel. Therefore, the element Al can pass through the barrier of the outer layer of the coating to diffuse outward to the oxidation area, and combine with O to form an Al_2O_3 oxide layer. Although the outer layer of the coating forms a channel for element diffusion, the diffusion rate of element Al weakens due to the loss of element Cr and the poor compactness of the coating, failing to supply sufficient Al. This results in the generation of numerous vacancies. A large number of vacancies accumulate to form Kirkendall holes, which grow and merge to form holes, as shown in Fig. 8c. After the holes merge, they expand into cracks (Fig.9), laying a hidden danger for the subsequent spalling of the oxidation

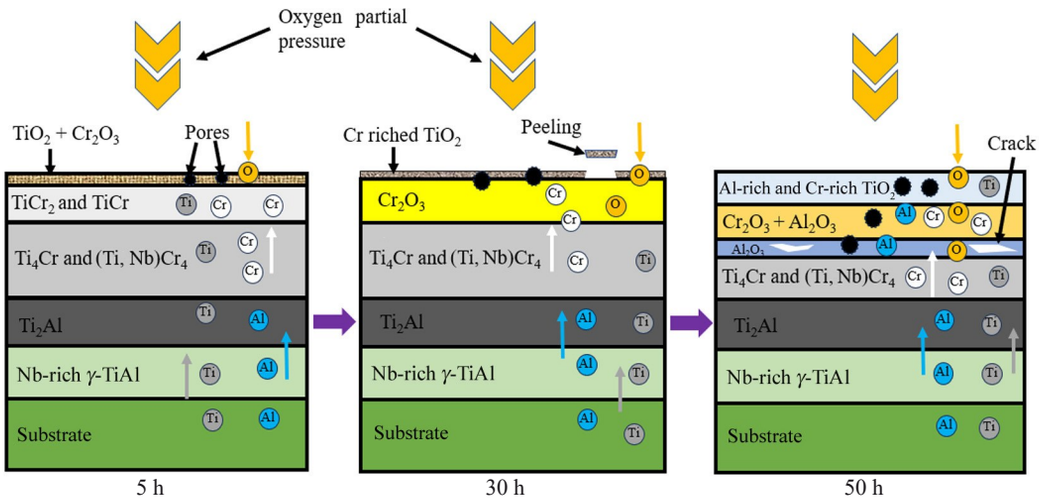

Fig.9 Schematic diagrams of microstructural evolution of Cr-Al-Y co-deposition coating after oxidation at 1273 K for different time

layer. The oxidation layer and the change process of the Cr-Al-Y coating at different oxidation time are shown in Fig.9.

4 Conclusions

1) The thickness of Cr-Al-Y co-deposition coating prepared by pack cementation at 1373 K for 2 h is about 30 μm, and it can be divided into three layers, including the outer layer, the inner layer, and Nb-rich γ-TiAl interdiffusion zone layer. The outer layer is composed of $TiCr_2$, TiCr, Ti_4Cr, and (Ti, Nb)Cr_4 phases. The inner layer is composed of Ti_2Al. The coating is uniform and dense, which maintains good metallurgical bonding with the substrate.

2) The TiAlNb9 alloy is oxidized at 1273 K to form an oxidation layer mainly containing TiO_2 and a small amount of Al_2O_3. The oxidation layer is loose and porous, accompanied by cracking and spalling, which cannot prevent the damage of element O to the alloy.

3) The oxidation products of Cr-Al-Y coating mainly include Cr_2O_3 and Al_2O_3. With the prolongation of oxidation time, the oxidation products accumulate to form a dense protective film, which effectively prevents the internal diffusion of element O. After oxidation at 1273 K for 50 h, the substrate can still be protected from oxidation erosion, which significantly improves the high-temperature oxidation resistance of TiAlNb9 alloy.

References

1 Fu Yu, Zhang Liwei, Wang Jiacheng *et al*. *Ceramics International*[J], 2023, 49(23): 37214

2 Kundu J, Chakraborty A, Kundu S. *Welding in the World*[J], 2020, 64(12): 1

3 Neelam N S, Banumathy S, Bhattacharjee A *et al*. *Corrosion Science*[J], 2019, 163: 108300

4 Li Yunyang, Yan Haojie, Wu Liankui *et al*. *Journal of Materials Research and Technology*[J], 2023, 27: 2882

5 Ye Chao, Chen Shijie, Liu Wei *et al*. *Metals*[J], 2022, 12(12): 2040

6 Rojas T C, Domínguez-Meister S, Brizuela M *et al*. *Surface and Coatings Technology*[J], 2018, 354: 203

7 Richter S, Glechner T, Wojcik T *et al*. *Surface and Coatings Technology*[J], 2024, 476: 130191

8 Wu Xiangqing, Xie Faqin, Tian Jin *et al*. *Rare Metal Materials and Engineering*[J], 2016, 45(12): 3144 (in Chinese)

9 Zhang Yang, Zhang Pingze, Chen Xiaohu *et al*. *Materials for Mechanical Engineering*[J], 2014, 38(4): 25 (in Chinese)

10 Li Yongquan, Xie Faqin, Wu Xiangqing. *Transactions of Nonferrous Metals Society of China*[J], 2015, 25(3): 803

11 Tian Jinlian, Hu Chun, Chen Li *et al*. *Transactions of Nonferrous Metals Society of China*[J], 2021, 31(9): 2740

12 He Jiayi, Liao Xuefeng, Lan Xuexia *et al*. *Journal of Alloys and Compounds*[J], 2021, 870: 159229

13 Li Yongquan, Li Xuan, Geng Guihong *et al*. *Tribology*[J], 2016, 36(6): 736 (in Chinese)

14 Li Yongquan, Tian Xingda, Wang Cunxi *et al*. *Rare Metal Materials and Engineering*[J], 2009, 24(6): 1219 (in Chinese)

15 Lin Naiming, Xie Faqin, Wu Xiangqing *et al*. *Journal of Rare Earths*[J], 2011, 29(4): 396

16 Kahrobaee Zahra, Palm Martin. *Journal of Alloys and Compounds*[J], 2022, 924: 166223

17 Yu Wenhai, Tian Jin, Tian Wei *et al*. *Journal of Rare Earths*[J], 2015, 33(2): 221

18 Li Yongquan, Xie Faqin, Wu Xiangqing *et al*. *Journal of Inorganic Materials*[J], 2013, 28(12): 1369 (in Chinese)

19 Wu X H, Huang A, Hu D *et al*. *Intermetallics*[J], 2009, 17(7): 540

20 Tian Shiwei, He Anrui, Liu Jianhua *et al*. *Materials Characterization*[J], 2021, 178: 111196

21 Pan Y, Lu X, Hu T L *et al*. *Journal of Materials Science*[J], 2020, 56(1): 1

22 Wei Xiangfei, Zhang Pingze, Wei Dongbo *et al*. *Rare Metal*

Materials and Engineering[J], 2022, 58(8): 1003

23 Zheng Liwei, Liu Enze, Zheng Zhi *et al*. *Corrosion Science*[J], 2023, 213: 110991

TiAlNb9合金表面Cr-Al-Y共渗层组织结构及高温氧化性能

郝清锐[1]，李涌泉[2,3]，李　宁[1]，高　阳[2]

(1. 北方民族大学 材料科学与工程学院，宁夏 银川 750021)

(2. 北方民族大学 机电工程学院，宁夏 银川 750021)

(3. 宁夏回族自治区复合制造系统工程技术研究中心，宁夏 银川 750021)

摘　要：为提高TiAlNb9合金的抗高温氧化性能，采用包埋渗的方法，在合金表面制备了Cr-Al-Y共渗层，通过扫描电子显微镜、能谱仪和X射线衍射仪分析了渗层的组织结构，对比研究了基体和渗层在1273 K下的高温氧化性能。结果表明：Cr-Al-Y共渗层约30 μm厚，结构致密，膜基结合较好，由外到内依次为由$TiCr_2$、TiCr、Ti_4Cr及(Ti, Nb)Cr_4相组成的外层，Ti_2Al内层及富Nb的γ-TiAl互扩散层。TiAlNb9基体在1273 K下生成TiO_2与Al_2O_3组成的氧化层，由于TiO_2形成的氧化膜结构疏松多孔，无法有效隔绝O元素的内扩散，致使基体不断受到氧化破坏。Cr-Al-Y渗层在氧化时会形成致密的Cr_2O_3和Al_2O_3氧化层，有效阻止了O元素的内扩散，显著提高了基体合金的抗高温氧化性能。

关键词：包埋渗；TiAlNb9合金；Cr-Al-Y共渗层；抗高温氧化

作者简介：郝清锐，男，1995年生，硕士生，北方民族大学材料科学与工程学院，宁夏 银川 750021，E-mail：1833737040@qq.com